

ac dynamics of ferroelectric domains from an investigation of the frequency dependence of hysteresis loops

S. M. Yang,¹ J. Y. Jo,¹ T. H. Kim,¹ J.-G. Yoon,² T. K. Song,³ H. N. Lee,⁴ Z. Marton,^{4,5} S. Park,⁶ Y. Jo,⁶ and T. W. Noh^{1,*}

¹*ReCFI, Department of Physics and Astronomy, Seoul National University, Seoul 151-747, Korea*

²*Department of Physics, University of Suwon, Hwaseong, Gyeonggi-do 445-743, Korea*

³*School of Nano and Advanced Materials Engineering, Changwon National University, Changwon, Gyeongnam 641-773, Korea*

⁴*Materials Science and Technology Division, Oak Ridge National Laboratory, Oak Ridge, Tennessee 37831, USA*

⁵*Department of Materials Science and Engineering, University of Pennsylvania, Philadelphia, Pennsylvania 19104, USA*

⁶*Division of Materials Science, Korea Basic Science Institute, Daejeon 305-333, Korea*

(Received 25 October 2010; published 30 November 2010)

We investigated the pinning dominated domain-wall dynamics under an ac field by studying the frequency (f) dependence of hysteresis loops of a uniaxial ferroelectric (FE) system. We measured the fully saturated polarization-electric field (P - E) hysteresis loops of high-quality epitaxial 100-nm-thick $\text{PbZr}_{0.2}\text{Ti}_{0.8}\text{O}_3$ capacitors at various f (5–2000 Hz) and temperatures T (10–300 K). We observed that the coercive field E_C is proportional to f^β with two scaling regions, which was also reported earlier in magnetic systems [T. A. Moore and J. A. C. Bland, *J. Phys.: Condens. Matter* **16**, R1369 (2004), and references therein]. In addition, we observed that the two scaling regions of E_C vs f exist at all measured T . We found that the existence of the two scaling regions should come from a dynamic crossover between the creep and flow regimes of the FE domain-wall motions. By extending the theory of Nattermann *et al.*, which was originally proposed for impure magnet systems [T. Nattermann, V. Pokrovsky, and V. M. Vinokur, *Phys. Rev. Lett.* **87**, 197005 (2001)], to the disordered FE systems, we obtained analytical expressions for the dynamic crossovers between the relaxation and creep, and between the creep and flow regimes. By comparing with the experimental data from our fully saturated P - E hysteresis loop measurements, we could construct a T - E dynamic phase diagram with f as a parameter for hysteretic FE domain dynamics in the presence of an ac field.

DOI: [10.1103/PhysRevB.82.174125](https://doi.org/10.1103/PhysRevB.82.174125)

PACS number(s): 77.80.Dj, 05.45.-a, 77.80.Fm

I. INTRODUCTION

The electric polarization (P)-electric field (E) hysteresis loop is a hallmark of ferroelectricity. By applying an alternating (ac) E , we can obtain the P - E hysteresis loop. This curve provides us with important ferroelectric (FE) information, including the remnant polarization P_r and the coercive electric field E_C . Therefore, many researchers perform P - E hysteresis measurements to investigate FE materials. However, the strongly nonlinear characteristics of the hysteresis loop still prevent some fundamental issues from being clearly understood. One such issue is the frequency (f) dependence of hysteresis loops: namely, how does the dynamic process of P reversal depend on the sweep rate of the external ac field? In addition, nowadays, understanding the f dependence of hysteresis loops has also become important technologically, since many nanoscale FE devices, such as nonvolatile memories and data storage, require operations at very high f .

In the P reversal process of a FE material, domains play an important role. Without an external E , the free energy of a FE material prefers the configuration consisting of domains, each having the same P direction. Under an external E , the volume of the favored domain state increases by the nucleation and subsequent growth of the domains.¹ Consequently, the detailed shape of the P - E hysteresis loop should be strongly affected by the nucleation and domain-wall (DW) motions. And time (t)-dependent behaviors of nucleation and DW motions should depend significantly on the experimental conditions, such as f , amplitude of the applied E (E_{max}), and

temperature T . As expected, the shape of the P - E hysteresis loop should be influenced by these experimental conditions. In particular, the E_C value has been known to have a strong f dependence.^{2,3} Therefore, the systematic studies on the f dependence of P - E hysteresis loops might provide us a useful way to obtain comprehensive understanding on the hysteretic dynamics of FE domains in the presence of an ac field.

There have been some theoretical and experimental efforts to understand the f dependence of P - E hysteresis loops.²⁻⁷ Up to this point, two theoretical models have commonly been used to explain the f dependence of hysteresis by using domain dynamics. Ishibashi and Orihara⁵ developed a phenomenological model which considered domain growth as the key process. They calculated the t -dependent fractional volume of reversed domains based on the extended Avrami theory.⁸ According to their model, E_C follows the simple power-law relationship, $E_C \propto f^\beta$. On the other hand, Du and Chen⁶ proposed a model to explain the f dependence of E_C which assumed that the limiting step is the nucleation process. Later, Jung *et al.*³ investigated experimentally the f dependence of E_C in various polycrystalline FE capacitors and compared their data with the Ishibashi-Orihara and Du-Chen models. They observed that both models fit the data reasonably well but the Du-Chen model was somewhat better at explaining their results. On the other hand, So *et al.*⁷ investigated the f dependence of E_C in epitaxial $\text{PbZr}_{0.4}\text{Ti}_{0.6}\text{O}_3$ capacitors. They obtained the $E_C \propto f^\beta$ relation, following the Ishibashi and Orihara model. At this point, we want to point out that the earlier works on the f dependence of the P - E hysteresis loops paid little attention to the roles of

quenched defects in FE disordered media, which are known to govern the nucleation^{9–11} and growth^{12–17} of domains.

In numerous materials, quenched defects will act as pinning centers for the movements of elastic objects, such as FE and ferromagnetic DWs, vortices in type II superconductors, charge-density waves, and dislocation lines.^{13,14,16,18,19} The physics on the growth of such elastic object in a disordered medium is known to be governed by the competition between the elastic energies and the pinning potentials of defects.^{13,16} Due to such competition, DW velocity v can have different E dependence. Depending on the magnitude of the constant (dc) E , there exist three regimes at finite T : pinned ($v=0$), creep (v has an exponential relationship), and flow regimes ($v \propto E$).^{16,18,19} Recent development of piezoresponse force microscopy (PFM) allowed us to measure the v - E relations directly in FE materials. Tybell *et al.*¹³ measured the DW velocities from the PFM images of epitaxial $\text{PbZr}_{0.2}\text{Ti}_{0.8}\text{O}_3$ films and demonstrated the existence of creep regimes in FE DW dynamics. Paruch *et al.*¹⁴ investigated the static configuration of the pinned DW and obtained the related roughness exponent. Quite recently, Jo *et al.*¹⁶ showed that the dc field driven DW dynamics, including creep, depinning, and flow motions, occurs in the real FE system under wide T and E ranges. However, all of these works have been focused on the DW dynamics under dc fields.^{13–16}

Up to our best knowledge, there has been no theoretical prediction to consider the effects of quenched defects on the f dependence of P - E hysteresis loop of the FE materials. On the other hand, for ferromagnetic systems, Nattermann *et al.*¹⁹ made theoretical studies on the magnetization (M)-magnetic field (H) hysteretic dynamics at finite T . They showed that the ferromagnetic DW subject to an ac field starts to move when the driving force exceeds an effective threshold field, which is T and f dependent. They evaluated the H_ω and H_T values where the dynamic crossovers from the relaxation to creep and from the creep to flow regimes, respectively, occur.²⁰ By using the predicted H_ω and H_T values, they made a T - H dynamic phase diagram for the relaxation, creep, and flow regimes of DW motion. Based on this pioneering work, there have been recent efforts to investigate experimentally the ac dynamics of ferroic DWs in FEs, FE relaxors, and ferromagnetics.^{21–25} In particular, Chen *et al.*²¹ measured the ac magnetic susceptibilities of $\text{Co}_{80}\text{Fe}_{20}/\text{Al}_2\text{O}_3$ multilayers and showed experimentally that ferromagnetic domains in a disordered medium experience the dynamic phase transitions among relaxation, creep, sliding, and switching. However, as pointed out in Ref. 21, it remains a challenge to discover the predicted T - H dynamic phase transitions from direct M - H hysteresis loop measurements. Considering the generality of the physics of domain growth in disordered media, we should be able to extend the theoretical work of Nattermann *et al.* to a FE system. If we build the T - E dynamic phase diagram directly from our P - E hysteresis loops, it can be an important step in obtaining full understanding of how elastic objects grow in a disordered medium under an ac driving force.

In this paper, we report our investigations on how the pinning dominated DW dynamics under an ac field will affect the f dependence of the hysteresis loops of a uniaxial FE system. In Sec. II, we describe experimental results on the

P - E hysteresis loops of a high-quality epitaxial $\text{PbZr}_{0.2}\text{Ti}_{0.8}\text{O}_3$ (PZT) thin film at various f and T . In Sec. III, by extending the theory of Nattermann *et al.* to the FE system, we obtained corresponding equations for dynamic crossovers between the relaxation and creep regimes, and between the creep and flow regimes, in a disordered FE system. We also discuss the case of the relaxation regime being absent when P is initially fully saturated. Finally, in Sec. IV, we discuss our experimental observations based on the theory, described in Sec. III. From the experimental findings, we constructed a dynamic T - E phase diagram for hysteretic ac domain dynamics, which agrees with the theoretical predictions.¹⁹

II. EXPERIMENTS AND RESULTS

We deposited a high-quality 100-nm-thick epitaxial PZT film on a $\text{SrRuO}_3/\text{SrTiO}_3$ (001) substrate by pulsed laser deposition. A metallic SrRuO_3 layer of 4 nm thickness was used as a bottom electrode. A more detailed description of the growth procedures has been published elsewhere.²⁶ X-ray diffraction studies confirmed that our film was composed of purely c -axis oriented domains, i.e., it had uniaxial symmetry and only 180° DW configurations.²⁶ For electrical measurements, we fabricated Pt top electrodes with a diameter of $100\ \mu\text{m}$ by using sputtering and photolithography lift-off process.

To investigate the f dependence of P - E hysteresis loops, we applied triangular waves with various f (i.e., 5–2000 Hz) to the PZT capacitors by means of a TF analyzer 2000 (aix-ACCT). We performed such measurements in a wide T range, i.e., 10–300 K. We determined the values of E_C to be $(|E_{C+}| + |E_{C-}|)/2$, where E_{C+} and E_{C-} are the positive and negative E_C in the P - E hysteresis loops, respectively. Note that the detailed shape of P - E hysteresis loop can be changed significantly depending on the magnitude of applied E . To avoid any artifacts possibly coming from the incomplete saturation, we always used E_{max} of a triangular wave at least 2.5 times larger than the corresponding E_C value for a given T . From this method, we could obtain fully saturated P - E hysteresis loops reliably.

Note that our epitaxial PZT films are very high quality with little leakage currents, so they are ideal for systematic ac measurements. Figure 1(a) shows the f -dependent hysteresis loops for the PZT film, measured at 300 K. At the lowest f , the hysteresis loop looked almost like a square, manifesting a high FE quality of our PZT film. They showed imprint, which might come from the different top and bottom electrodes. However, it is negligibly small, i.e., less than 0.04 MV/cm. As shown in the inset, the thin film is also highly insulating with nearly zero leakage current.

We found that the P - E hysteresis loop experiences systematic f -dependent changes near E_C . As shown in Fig. 1(a), E_C increases and the slope at E_C decreases with increases in f . In other words, the squarelike loop at 50 Hz becomes very slanted one at 2000 Hz. This systematic change indicates that the DW dynamics around E_C should play a major role in the f -dependent shape change in hysteresis loops.

To obtain further insights, we checked whether $E_C \propto f^\beta$, as predicted by the Ishibashi-Orihara model.⁵ Figure 1(b) shows

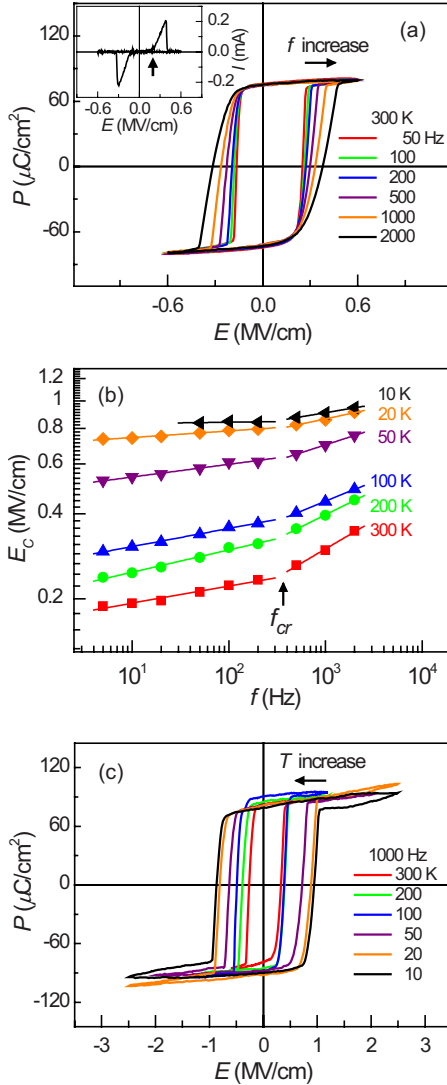


FIG. 1. (Color online) (a) f -dependent P - E hysteresis loops of the PZT film at 300 K. The inset shows the switching current I - E curve at $f=1000$ Hz. (b) The E_C values as a function of f at various T . The f_{cr} indicates the crossover frequency where two scaling regions are separated. The solid lines show the linear fitting results for each f region. (c) T -dependent P - E hysteresis loops at $f=1000$ Hz.

the plot of $\log E_C$ vs $\log f$. As shown by the first bottom (red) linear fitting line, the E_C data at 300 K can be fitted with the relation of $E_C \propto f^\beta$ quite successfully. This agreement is consistent with the earlier works that the DW movement, rather than the domain nucleation, should play an important role in the domain switching of epitaxial thin films.^{7,15} Intriguingly, the log-log plot of E_C and f displays two scaling regimes. Namely, the increase in E_C becomes much stronger at the higher f . And the crossover between two regimes occurs around 200–500 Hz.

We found that T also significantly affects the shape change in the P - E hysteresis loops. Figure 1(c) shows T -dependent hysteresis loops for the PZT film at $f=1000$ Hz. Contrary to the f dependence, the slope at E_C did not change significantly and the general shape of the P - E

hysteresis loops remains similar. However, as T increased, there were distinctive decreases in E_C . This sharp decrease suggests that the P switching in the FE film should be strongly affected by thermal processes.

We also found that the behavior of two scaling regimes does exist for all measured T , as displayed in Fig. 1(b). For all T between 10 and 300 K, we observed two scaling regions with different β values. It should be noted that the crossover frequency f_{cr} remains to be nearly constant, i.e., 200–500 Hz, for all measured T . This indicates the f_{cr} value should have a rather weak T dependence. Although the two scaling regimes of E_C vs f at room T were observed in epitaxial $\text{PbZr}_{0.4}\text{Ti}_{0.6}\text{O}_3$ capacitors,⁷ their origin is still unclear. On the other hand, for magnetic systems, there have been reports on the behavior of two scaling regimes.^{21,27,28} They explained that the two scaling regimes come from the competition between different domain processes, such as DW motion and nucleation,^{21,27,28} or the crossover between thermally activated and viscous processes driving the DW motions.^{27,28} We argue that the existence of two scaling regimes should be closely related to the ac FE DW dynamics. In Sec. IV, we will show how the dynamic crossover between the creep and flow motions can affect this f dependence of E_C .

III. THEORETICAL WORK ON THE ac DYNAMICS OF DWS

As mentioned in Sec. I, Nattermann *et al.*¹⁹ developed a theory which explains how the hysteresis loop of impure ferromagnetic systems can be varied by the amplitude and f of an external ac H field based on the quenched Edwards-Wilkinson equation.²⁹ Although their original description was limited to the hysteretic motion of ferromagnetic domains, it can be applied to other ferroic systems due to the generality of the related physics. Therefore, in this section, we will extend the theory of Nattermann *et al.* to the FE system and obtain some related equations for ac FE DW dynamics.

Figure 2(a) shows a dynamic phase diagram for the DW hysteretic motions under an ac field at finite T and f , as predicted by Nattermann *et al.*¹⁹ The vertical solid (red) E_1 and (blue) E_2 lines indicate the dynamic crossover lines, separating between the relaxation and creep, and between the creep and flow regimes, respectively. The horizontal (green) $E(t)$ line shows the first $1/4f$ of $E(t)$ during the P - E hysteresis loop measurements. The f dependence of the P - E hysteresis loop measurements correspond to how fast the $E(t)$ line sweeps. The dotted (black) line separates the critical depinning region from other dynamic regimes at low T . However, in this paper, we will focus on two dynamic crossovers, i.e., between relaxation and creep, and between creep and flow regimes.

A. Dynamic crossover between the relaxation and creep regimes (E_{depin})

As displayed schematically in the bottom solid curve of Fig. 2(b), when the DWs exist initially, there should be en-

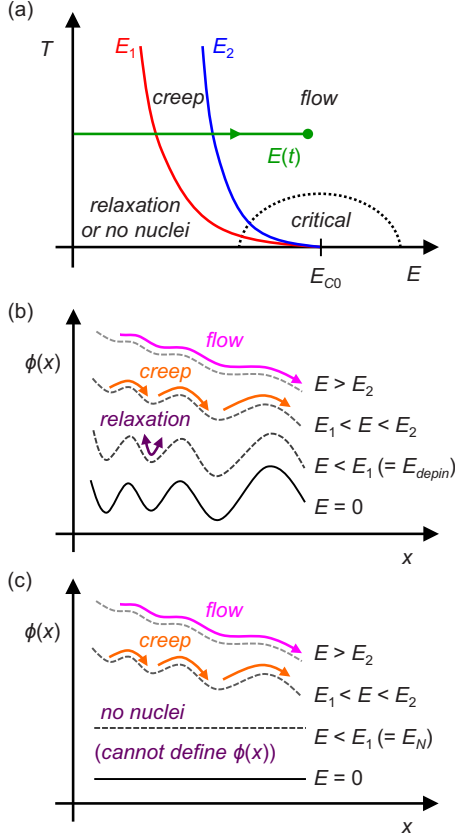


FIG. 2. (Color online) (a) The dynamic phase diagram for the DW hysteresis under an ac field at finite T and f . The vertical solid lines (red) E_1 and (blue) E_2 indicate the dynamic crossover lines separating the relaxation, creep, and flow regimes. The horizontal (green) line indicates the first $1/4f$ of $E(t)$ during the P - E hysteresis loop measurements. Schematic of energy landscapes $\phi(x)$ (the solid line) and various DW motions depending on the E in random media during the first $1/4f$, (b) when DWs exist initially and (c) when they do not exist initially.

ergy landscapes $\phi(x)$ which varies from place to place in a disordered FE medium. The sites with the local energy minima act as the pinning sites where quenched defects probably exist. Due to the random nature of these pinning sites, there is a wide distribution of energy barrier heights U_B . Under the sweep of an external $E(t)$, the $\phi(x)$ should change, resulting in the dynamic crossover of the DW motions.

In the *creep* regime, the thermally activated hopping will induce DW movements from one local minimum to the next, as shown by the (orange) arrows in the second top curve of Fig. 2(b).^{13,18,19} This creep motion should be governed by the maximum energy barrier $U_{B,max}$. To overcome $U_{B,max}$ by thermal activation, a certain hopping time τ is required,¹⁹

$$\tau \approx \tau_0 \exp(U_{B,max}/k_B T), \quad (1)$$

$$U_{B,max} \approx U(E_{C0}/E)^\mu (1 - E/E_{C0})^\eta, \quad (2)$$

where τ_0 , U , and E_{C0} are a microscopic hopping time, a characteristic pinning energy, and a depinning threshold field at $T=0$, respectively. Note that μ is a dynamical exponent,

which mirrors both the dimension and the nature of disorder (e.g., random bonds or random fields) of the system.¹⁸ And η is an exponent related to the E dependence of the energy barrier.^{19,30} In order for the creep motion to occur, the hopping time τ should become smaller than $1/f$.

On the other hand, under a very weak E , called the *relaxation* regime, the creep motion cannot occur due to the long τ value. In other words, since the effective $U_{B,max}(E)$ is quite large and so τ becomes very long, it is impossible to overcome $U_{B,max}$ during one period (i.e., $\tau > 1/f$). There will be no effective DW motion, namely, $v=0$. In this case, the DW segments oscillate between the metastable states, as shown by the (purple) arrow in the second bottom line of Fig. 2(b).¹⁸ From the condition of $\tau f=1$ and Eqs. (1) and (2), we can evaluate the dynamic crossover E_{depin} between relaxation and creep regime,¹⁹

$$E_{depin}/E_{C0} = [(U/k_B T \Lambda)(1 - E_{depin}/E_{C0})^\eta]^{1/\mu}, \quad (3)$$

where $\Lambda = \ln(1/f\tau_0)$. When the DW exists initially, the E_{depin} plays the role of E_1 , as described in Fig. 2(b).

B. Dynamic crossover between the no nuclei and creep regimes (E_N)

However, when P is fully saturated initially, there are no existing domains of reversed P . Then, we should first consider the domain nucleation process. Figure 2(c) shows a schematic of how the DW motions will change when the DWs do not exist initially. In this case, the energy landscapes $\phi(x)$ for DW motion cannot be defined. Domain nucleation with an opposite P will occur at a certain field E_N required for overcoming the nucleation energy barrier U_N . Above E_N , the U_N can be overcome by thermal activation,³¹ and so the reversed domains are created. Note that the E_N value is generally larger than the E_{depin} value in the epitaxially grown film with uniaxial symmetry.¹⁷ Therefore, for $E > E_N$, the reversed domain nucleates and moves by thermally activated creep motion, as shown in Fig. 2(c). In this case, E_N plays the role of E_1 , determining the initiation of creep motion. There should be a *no nuclei* regime instead of a relaxation regime for $E < E_1$.

C. Dynamic crossover between the creep and flow regimes (E_2)

With increase in E , the effective $U_{B,max}$ becomes smaller and finally nearly negligible. Then, the DWs experience the viscous *flow* motion, as shown by the (magenta) arrow in the first top lines of Figs. 2(b) and 2(c). It is known that the velocity in the flow regime is linearly proportional to the external E , i.e., $v \propto \gamma E$, where γ is the effective friction coefficient.^{18,19} On the other hand, in the creep regime, the average velocity $v(E)$ should be linearly proportional to $1/\tau$ so^{18,19}

$$v \approx \gamma E \exp[-(U/k_B T)(E_{C0}/E)^\mu (1 - E/E_{C0})^\eta]. \quad (4)$$

Therefore, we can obtain the dynamic crossover value E_2 , separating the creep and flow regimes by comparing the $v \propto \gamma E$ with Eq. (4),¹⁹

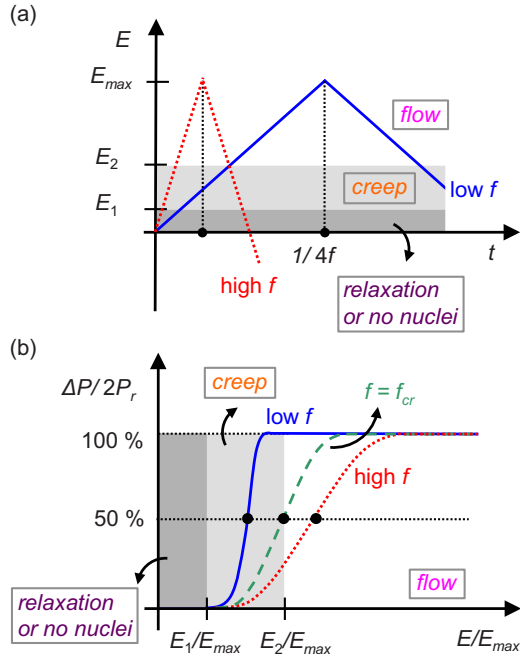


FIG. 3. (Color online) (a) Schematic of triangular waves of low f (the solid blue line) and high f (the dotted red line) used for measuring hysteresis loops. (b) Schematic of $\Delta P/2P_r$ as a function of E/E_{max} , where P_r is the remnant polarization. Solid circles show the values of E_C . The dashed (green) line shows the E -dependent $\Delta P/2P_r$ value at $f=f_{cr}$. The dark gray, gray, and white regions indicate the relaxation or no nuclei, creep, and flow regimes, respectively.

$$E_2/E_{C0} = [(U/k_B T)(1 - E_2/E_{C0})^\eta]^{1/\mu}. \quad (5)$$

As shown by vertical solid lines in Fig. 2(a), both E_1 and E_2 are monotonously decreasing functions of T with a maximum E_{C0} at $T=0$.

IV. DISCUSSION

A. Origin of two scaling E_C regions with f

For both cases, whether the DWs exist initially or not, there should be three regimes for FE DW motions in one cycle, as shown in Figs. 2(b) and 2(c). (1) At $E < E_1$, the motion will be either in the no nuclei or relaxation regime. (2) At $E_1 < E < E_2$, the DW moves by thermally activated creep motion. (3) At $E > E_2$, the DW undergoes a viscous flow motion.

When we apply an ac field with $E_{max} \gg E_C$, as shown in Fig. 3(a), the E value will vary in time during one period. The solid (blue) line and the dotted (red) line indicate the triangular waves at low f and high f , respectively. Note that E_1 separates the regimes between the relaxation (or no nuclei) and creep, and E_2 divides the flow regime from the creep regime. The dark gray, gray, and white regions show the relaxation (or no nuclei), creep, and flow regimes, respectively. As displayed in Fig. 3(a), the relative time duration that the FE system stays in each regime will vary depending on f . As f is lower, the time for one period becomes longer and so the relative time duration to stay in the relaxation (or

no nuclei) and creep regimes becomes also longer.

The shape of hysteresis loops is significantly affected by the dynamic crossovers between these three regimes of DW motion. Figure 3(b) shows the polarization reversal (ΔP) during the first $1/4f$. For low f , as represented by the solid (blue) line, the system will stay in the creep regime long enough to induce most of the ΔP . Since E_C is the E value at which 50% of ΔP occur, $E_C < E_2$ for low f . Then all of the ΔP should occur in a rather narrow region of E , which results in the nearly squarelike hysteresis observed in Fig. 1(a). This corresponds to the case where P switching process can occur at relatively small fields by the creep motion if enough time is given. On the other hand, for high f , E increases quickly in time, so the system will only remain in the creep regime for a rather short time and then transit to the flow regime, as shown by the dotted (red) line. In this case, the DW motions in the flow regime will induce most of the ΔP , so $E_C > E_2$. Since a rather large E region is required to complete ΔP , the hysteresis loop should be slanted, as shown in Fig. 1(a).

We therefore argue that the f -dependent variation in the contribution of DW motion to the P switching process should result in the two E_C scaling regions observed in Fig. 1(b). As shown by the dashed (green) line in Fig. 3(b), let us choose f_{cr} as the frequency where E_C becomes the same as the dynamic crossover value E_2 , i.e., $E_2 = E_C(f_{cr})$. Then if $f < f_{cr}$, the DW creep motion plays the major role in the P switching. On the other hand, if $f > f_{cr}$, the viscous flow motion will dominate.

B. Experimental determination of E_2

By using the above argument that $E_2 = E_C(f_{cr})$, we could measure experimentally the dynamic crossover value $E_2(T)$ at all measured T . First, we need to check the argument that $E_2 = E_C(f_{cr})$. Thus, we compared the experimental E_C values at f_{cr} with the predicted E_2 value in Eq. (5). The symbols in Fig. 4(a) show the experimental values of $E_C(f_{cr})$ as a function of T . As T increased, $E_C(f_{cr})$ decreased. As shown in Eq. (5), there are four parameters. First, it is known that $\eta=2$ at $T=0$.^{19,30} Second, for similarly prepared PZT capacitors, our earlier dc dynamics study showed that $E_{C0} \sim 1.0$ MV/cm, $U/k_B \sim 300$ K, and $\mu \sim 0.9$ (Ref. 16). Thus, without any free fitting parameters, Eq. (5) gives the solid line in Fig. 4(a), providing a good agreement with the experimental $E_C(f_{cr})$ values below 50 K. On the other hand, η can be different with 2 at finite T since η is known to be nonuniversal.¹⁹ Thus, for the high T region (100–300 K), we did another fit using η as a free fitting parameter. The higher T data fit quite well with $\eta=4.0 \pm 0.5$, as represented by the dashed line. These agreements validate our argument that the two scaling regions separated by $E_2 = E_C(f_{cr})$, and the f dependence of E_C originates from the dynamic crossover of DW motion between the creep and flow regimes. Therefore, the experimental value of $E_C(f_{cr})$ provides us with the dynamic crossover value E_2 .

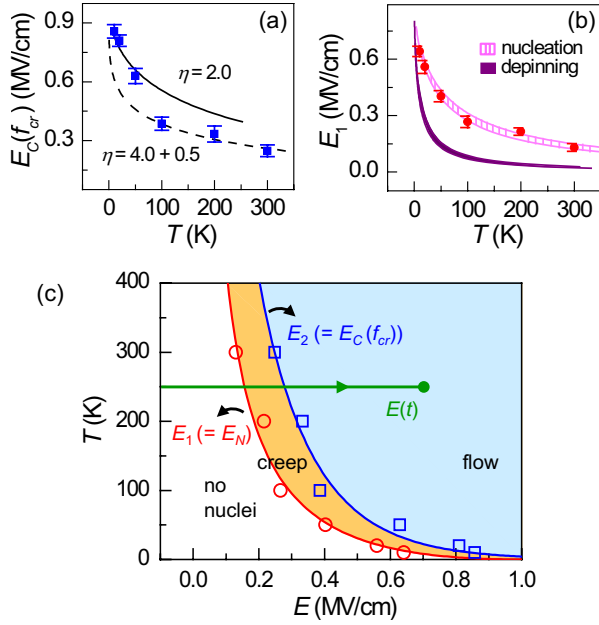


FIG. 4. (Color online) (a) Experimental values of $E_C(f_{cr})$ as a function of T . The solid and dashed lines indicate the fitting results using Eq. (5) with $\eta=2.0$ and about 4.0, respectively. (b) Experimental values of E_1 as a function of T . The solid (purple) and dashed (magenta) regions indicate the expected E_1 values by assuming the depinning process and domain nucleation process, respectively. (c) The dynamic phase diagram for ac FE domain dynamics, determined from the fully saturated P - E hysteresis loops. The (red) line E_1 and (blue) line E_2 separate the no nuclei, creep, and flow regimes.

C. Experimental determination of E_1

To construct the T - E dynamic phase diagram experimentally from the fully saturated P - E hysteresis loops, we consider now the remaining dynamic crossover value E_1 , which determines the initiation of the creep motion. We should determine whether there should be a no nuclei or a relaxation regime below E_1 . In other words, which schematic is valid between Figs. 2(b) and 2(c)? As shown in Fig. 3(b), E_1 could be measured by the value where ΔP increases rapidly. However, as shown in Fig. 1(a), it is difficult to estimate directly the E_1 values from the P - E hysteresis loops due to steep curvatures. To find out E_1 values clearly, we measured E_1 by using the E value where the switching current I started to increase significantly, as marked by the arrow in the inset of Fig. 1(a). The symbols in Fig. 4(b) display the experimental E_1 values as a function of T .

If E_1 is governed by depinning of the DWs, as described in Fig. 2(b), E_1 should correspond to E_{depin} . Using Eq. (4) and the value of $1/\tau_0 \sim 10^{13}$ Hz, i.e., the attempt frequency for a typical phonon,¹¹ we estimated the predicted E_{depin} values, as shown by the solid (purple) region in Fig. 4(b). The estimated E_{depin} values are dispersed not on a line but in a region because E_{depin} depends on f . However, our measured E_1 values are plotted far away from the predicted region of E_{depin} values. Therefore E_1 should not be considered as the dynamic crossover between the relaxation and creep regimes for the fully saturated P - E hysteresis experiments.

Let us check the other possibility that E_1 might result from the domain nucleation process, as described in Fig. 2(c). Practically, we fully saturated our PZT capacitors before the P - E hysteresis loop measurements. So the reversed domains should be nucleated before making any contribution such as depinning process of the DWs. To create the reversed domain nuclei, the nucleation energy barrier U_N should be also overcome by thermal activation.³¹ So we substituted U_N for U in Eq. (3) and obtained a good fit for the E_1 values, as represented by the dashed (magenta) region in Fig. 4(b). We found $U_N/k_B \sim 1800$ K, which is about six times larger than U/k_B . Since our PZT film was epitaxially grown and composed of only c domains, it is more reasonable that U_N is higher than U . Furthermore, the obtained U_N value is consistent with those ($U_N/k_B \sim 1200$ – $24\,000$ K) from the recent PFM study on the energy distribution of nucleation centers in PZT films.¹¹ Therefore, we concluded that the E_1 value is governed by the nucleation process, i.e., E_N in our P - E hysteresis loop measurements.

D. Construction of the T - E dynamic phase diagram

From these experimental findings, we constructed the dynamic phase diagram in the T vs E plane for ac field driven domain dynamics. As displayed in Fig. 4(c), this T - E dynamic phase diagram resembles that in Fig. 2(a). One difference is the existence of the no nuclei regime below E_1 . It comes from the initial poling process in our P - E hysteresis loop measurements, which makes all P in the film have the same orientation. The (red) circles and (blue) squares represent experimental E_1 and E_2 values, respectively. The lines are guidelines for eye. We could determine the values of E_1 as E_N , and the values of E_2 as $E_C(f_{cr})$.

Note that the horizontal (green) line indicates the first $1/4f$ of $E(t)$ during the P - E hysteresis loop measurements. Depending on how fast it moves, i.e., the change in f , the ΔP of the PZT capacitors is achieved mainly by either the creep or flow motion, as shown in Fig. 3(b). This difference in dominant DW dynamics determines the f dependence of hysteresis loops. This work presents a useful way to obtain ac domain dynamic information from the fully saturated P - E hysteresis loops of epitaxial FE thin films.

V. SUMMARY

We investigated the f dependence of P - E hysteresis loops of a high-quality epitaxial $\text{PbZr}_{0.2}\text{Ti}_{0.8}\text{O}_3$ film at 10–300 K. We observed that the DW dynamics around E_C plays an important role in the f -dependent shape change in hysteresis loops. Thermally activated creep motion is more dominant to P switching at low f while viscous flow motion at high f . This difference in the dominant mode of DW motion results in the two scaling regions of E_C with f . From this fact, we could measure the experimental dynamic crossover value $E_2(T)$. We also obtained another dynamic crossover value $E_1(T)$ from the switching current data. The E_1 values are governed by the nucleation process in our hysteresis loop measurements. Finally, we could construct the T - E dynamic phase diagram for the fully saturated P - E hysteresis mea-

surements. This work can be generalized to many ferroic systems, which are described by pinning dominated driven dynamics of elastic media in random environments.

ACKNOWLEDGMENTS

This research was supported by the National Research

Foundation of Korea (NRF) grant funded by the Korea government (MEST) (Grants No. 2009-0080567 and No. 2010-0020416). The work at Oak Ridge National Laboratory (H.N.L.) was sponsored by the Division of Materials Sciences and Engineering, Office of Basic Energy Sciences, U.S. Department of Energy.

*Author to whom correspondence should be addressed; twnoh@snu.ac.kr

- ¹M. Dawber, K. M. Rabe, and J. F. Scott, *Rev. Mod. Phys.* **77**, 1083 (2005).
- ²J. F. Scott, *Ferroelectric Memories* (Springer, Berlin, 2000).
- ³D. J. Jung, M. Dawber, J. F. Scott, L. J. Sinnamon, and J. M. Gregg, *Integr. Ferroelectr.* **48**, 59 (2002).
- ⁴R. Landauer, D. R. Young, and M. E. Drougard, *J. Appl. Phys.* **27**, 752 (1956).
- ⁵Y. Ishibashi and H. Orihara, *Integr. Ferroelectr.* **9**, 57 (1995).
- ⁶X. Du and I. W. Chen, *Ferroelectric Thin Film VI*, MRS Symposia Proceedings No. 493 (Materials Research Society, Pittsburgh, 1998), p. 311.
- ⁷Y. W. So, D. J. Kim, T. W. Noh, J.-G. Yoon, and T. K. Song, *Appl. Phys. Lett.* **86**, 092905 (2005).
- ⁸M. Avrami, *J. Chem. Phys.* **9**, 177 (1941).
- ⁹G. Gerra, A. K. Tagantsev, and N. Setter, *Phys. Rev. Lett.* **94**, 107602 (2005).
- ¹⁰D. J. Kim, J. Y. Jo, T. H. Kim, S. M. Yang, B. Chen, Y. S. Kim, and T. W. Noh, *Appl. Phys. Lett.* **91**, 132903 (2007).
- ¹¹S. Jesse, B. J. Rodriguez, S. Choudhury, A. P. Baddorf, I. Vrejoiu, D. Hesse, M. Alexe, E. A. Eliseev, A. N. Morozovska, J. Zhang, L. Q. Chen, and S. V. Kalinin, *Nature Mater.* **7**, 209 (2008).
- ¹²S. Hong, E. L. Colla, E. Kim, D. V. Taylor, A. K. Tagantsev, P. Muralt, K. No, and N. Setter, *J. Appl. Phys.* **86**, 607 (1999).
- ¹³T. Tybell, P. Paruch, T. Giamarchi, and J. M. Triscone, *Phys. Rev. Lett.* **89**, 097601 (2002).
- ¹⁴P. Paruch, T. Giamarchi, and J. M. Triscone, *Phys. Rev. Lett.* **94**, 197601 (2005).
- ¹⁵S. M. Yang, J. Y. Jo, D. J. Kim, H. Sung, T. W. Noh, H. N. Lee, J. G. Yoon, and T. K. Song, *Appl. Phys. Lett.* **92**, 252901 (2008).
- ¹⁶J. Y. Jo, S. M. Yang, T. H. Kim, H. N. Lee, J. G. Yoon, S. Park,

Y. Jo, M. H. Jung, and T. W. Noh, *Phys. Rev. Lett.* **102**, 045701 (2009).

- ¹⁷S. M. Yang, J. W. Heo, H. N. Lee, T. K. Song, and J.-G. Yoon, *J. Korean Phys. Soc.* **55**, 820 (2009).
- ¹⁸W. Kleemann, *Annu. Rev. Mater. Res.* **37**, 415 (2007).
- ¹⁹T. Nattermann, V. Pokrovsky, and V. M. Vinokur, *Phys. Rev. Lett.* **87**, 197005 (2001).
- ²⁰In the relaxation regime, the net DW motion does not occur, i.e., $v=0$, under an ac field, as described in Ref. 18. It corresponds to the pinned regime under a dc field.
- ²¹X. Chen, O. Sichelshmidt, W. Kleemann, O. Petravic, C. Binek, J. B. Sousa, S. Cardoso, and P. P. Freitas, *Phys. Rev. Lett.* **89**, 137203 (2002).
- ²²O. Petravic, A. Glatz, and W. Kleemann, *Phys. Rev. B* **70**, 214432 (2004).
- ²³W. Kleemann, J. Dec, S. A. Prosandeev, T. Braun, and P. A. Thomas, *Ferroelectrics* **334**, 3 (2006).
- ²⁴W. Kleemann, J. Rhensius, O. Petravic, J. Ferre, J. P. Jamet, and H. Bernas, *Phys. Rev. Lett.* **99**, 097203 (2007).
- ²⁵T. Braun, W. Kleemann, J. Dec, and P. A. Thomas, *Phys. Rev. Lett.* **94**, 117601 (2005).
- ²⁶H. N. Lee, S. M. Nakhmanson, M. F. Chisholm, H. M. Christen, K. M. Rabe, and D. Vanderbilt, *Phys. Rev. Lett.* **98**, 217602 (2007).
- ²⁷B. Raquet, R. Mamy, and J. C. Ousset, *Phys. Rev. B* **54**, 4128 (1996).
- ²⁸T. A. Moore and J. A. C. Bland, *J. Phys.: Condens. Matter* **16**, R1369 (2004).
- ²⁹S. F. Edwards and D. R. Wilkinson, *Proc. R. Soc. London, Ser. A* **381**, 17 (1982).
- ³⁰A. A. Middleton, *Phys. Rev. B* **45**, 9465 (1992).
- ³¹J. Y. Jo, D. J. Kim, Y. S. Kim, S. B. Choe, T. K. Song, J. G. Yoon, and T. W. Noh, *Phys. Rev. Lett.* **97**, 247602 (2006).